Indian Journal of Advances in Chemical Science

Article

# Titanium Dioxide Enhanced Manganese Phosphate Chemical Conversion Coating on D2 Steel at Various Concentrations

**M. Padma[1,2], K. Ravichandran[1]***

*[1]Department of Analytical Chemistry, University of Madras, Guindy, Chennai, Tamil Nadu, India, [2]Department of Chemistry, Bharathi Women's College, Chennai, Tamil Nadu, India*

**ABSTRACT**

We exercised iron-manganese phosphate composite coatings to defend the surface of D2 steel from corrosion. Addition of titanium dioxide (additive) in different concentrations to the phosphating solution made significant difference in coating weight, coating time, morphology, porosity, and anti-corrosion performance of phosphate chemical conversion coating on D2 steel was studied. The resultant coatings were characterized by field emission scanning electron microscopy, energy-dispersive X-ray analysis, and X-ray diffraction measurements to ascertain the morphological features, chemical composition, and phase constituents, respectively. The corrosion resistance of coated samples in 3.5% NaCl was evaluated by potentiodynamic polarization and electrochemical impedance spectroscopy. Potential time measurement helped to track the phosphate coating formation and offer an indication about completion of coating process. The results infer that the presence of additive could be formed highly corrosion resistant phosphate composite coatings. It is an approach to determine the optimum concentration of additive which provides better protective layer.

**Key words:** Phosphate chemical conversion coating; Titanium dioxide; Corrosion resistance and coating completion time.

## 1. INTRODUCTION

Phosphate chemical conversion (PCC) coating is a widely adopted treatment in automobile industry for many purposes such as corrosion resistance, anti-friction, oil-affusing, electric insulation, and so on [1]. Most automobile bodies are zinc phosphated before painting to increase corrosion resistance and paint adhesion. To improve the corrosion resistance, a dense, finely structured, and firm phosphate composite coating has been developed on the bare metal [2]. Manganese phosphate coating has the highest hardness and superior corrosion resistance than the zinc phosphate coating [3]. Although PCC coating has been remarked as the best choice for a large percentage of steel and iron ordnance components which demands excellent corrosion resistance [4,5], it has failed to meet certain industrial applications due to presence of some intrinsic micro defects [6]. Therefore, recently, some specific non-ferrous metal oxides have been introduced into the PCC coating system [6,7] to improve the corrosion resistance of coated material.

Titanium dioxide is used in many applications due to its opacity, high chemical stability, good weather resistance, best dispersibility, and brightness. It's been used in printing inks, plastics, paper, paints, and coating industries. Titanium dioxide as an additive has improved the ability of surface coating in terms of particle size, particle size distribution, lattice stabilization, morphological features, chemical composition, and corrosion behavior. A well-dispersed system helps to develop coatings with improved thickness and high weather durability.

## 2. MATERIALS AND METHODS

### *2.1. Materials and Deposition Methodology*

Commercially obtained D2 steel was used as samples (composition in wt.%: C-0.17, Si-0.07, Mn-0.60, Co-1.00, P-0.03, S-0.03, Mo-0.70, Cr-11.00, Cu-0.25, Ni-0.30, and Fe-Balance) with the dimensions of 5 cm × 8 cm × 0.2 cm. The samples were polished, degreased, and allowed to acid pickling followed by washing and drying. Phosphating solution (electrolyte) consists of 6.9 g/L of manganese carbonate, 6 ml/L of orthophosphoric acid (85%), and 1.5 ml/L of conc. nitric acid (70%). pH of the phosphate solution was roughly 2.83 and 90°C temperature was maintained constantly using oil bath. Experiment was repeated 3 times to ensure the concordant coating weight.

### *2.2. Mass Measurement of Phosphated Layer*

Mass of phosphate composite coating employed on D2 steel was calculated from the weight difference. Triplicate samples were subjected to coating and used to calculate the coating weight and the average values were plotted. The specific mass of the phosphated layer and ion dissolution per unit area can be expressed using the formulae [7,8].

$$M_{\text{Phosphated layer}} = \frac{W_2 - W_3}{A} g / m^2$$

$$\text{Ion Dissolution} = \frac{W_1 - W_3}{A} g / m^2$$

Where, $W_1$ – weight of base metal, $W_2$ – weight of phosphate layer, $W_3$ – weight of the sample after removing coated film, and A – the surface

***Corresponding author:**
*E-mail: raavees@unom.ac.in.*

**ISSN NO:** 2320-0898 (p); 2320-0928 (e)
**DOI:** 10.22607/IJACS.2021.901003

**Received**: 18th December 2020;
**Revised:** 02nd January 2020;
**Accepted:** 02nd January 2020

area of phosphated sample. ($W_1$, $W_2$, and $W_3$ were averaged over three measurements).

Surface morphology was analyzed by flame emission SEM (FE-SEM) (Instrument : SU6600, S.No. HI-2108-0002) while their chemical composition was determined by energy-dispersive X-ray analysis (EDX) enclosed with the FE-SEM. The phase content of the coated film was revealed by X-ray diffraction (XRD) measurements using Cu Kα radiation (Bruker Model D8).

### *2.3. Evaluation of Corrosion Resistance*

Corrosion resistance of phosphate composite coatings in 3.5% NaCl was examined by potentiodynamic polarization and electrochemical impedance spectroscopy (EIS) studies (Instrument: Electrochemical workstation, CHI660B). Potentiodynamic polarization measurements were studied in the potential range from −250 mV(SCE) in the cathodic direction to +1000 mV (SCE) in the anodic direction from open circuit potential (OCP) at the scan rate of 100 mV/min. To make sure the results, experiment was repeated 3 times. EIS studies were predicted at their respective OCPs. From the Nyquist plot, EIS parameters could be obtained after fitting the data using ZSimpWin 3.21 software.

## 3. RESULTS AND DISCUSSION

### *3.1. PCC Coating on D2 Steel*

PCC coating has been carried out on ferrous metal. When sample is placed into the phosphating solution, a topochemical reaction occurs [9]. At microanodic sites, $Fe^{2+}$ ions subsequently react with $Mn^{2+}$ and $PO_4^{3-}$ to form iron-manganese phosphate composite named as hureaulite $[Mn.Fe)_5.H_2(PO_4)_4.4H_2O]$. At the cathodic sites, certain amount of the $Fe^{3+}$ ions reduced to $Fe^{2+}$ ions and rest of the $Fe^{3+}$ ions react with $PO_4^{3-}$ ions to form $FePO_4$. The solubility product of $FePO_4$ is very low (Ksp : $1.3 \times 10^{-22}$ at 25°C) hence it gets precipitate as sludge.

The change in pH modifies hydrolytic equilibrium (between the soluble primary phosphates and the insoluble tertiary phosphates) resulting in the speedy deposition of various types of insoluble tertiary phosphates [4,7]. The $NO_3^-$ ions reduced at microcathodes favor the rate of deposition. Mass of phosphated layer and the respective amount of ion dissolution of coated samples are plotted in Figure 1, shown in Table 1. Hydrogen evolution occurred throughout the process indicates the presence of metallic sites (Fe) on the surface. It is also observed that the deposition of Fe occurs in the form of fixed channels while the manganese phosphate deposit on adjacent areas [10].

### *3.2. Characteristics of Coated Sample*

The surface morphology and chemical composition of coated samples are shown in Figure 2. The coatings are compact and uniform flower like particles confirmed by morphological studies. However, the particles of untreated sample were larger in size (≈40 µm) than that of treated sample (≈10 µm) which increase the number of particles deposited thus avoiding the voids formation at the maximum. Hence, the coating of treated samples was denser and less porous compared with untreated sample. EDX spectra proved that O, P, Mn, and Fe [9] are predominant elements and also revealing that the amount of these

**Table 1:** Coating weight, Ion dissolution, Electrochemical parameters, Corrosion weight and Corrosion rate (Instrumentally) of $TiO_2$ assisted PCC coating.

| Conc. of additive (g/L) | Coating weight ($g/m^2$) | Ion Dissolution ($g/m^2$) | Ecorr V (SCE) | Icorr ($\mu A.cm^{-2}$) | Rs ($\Omega.cm^2$) | CPE ($\mu A.cm^{-2}$) | n | $R_1$ ($\Omega.cm^2$) | Corrosion weight ($g/m^2$) | Corrosion rate (g/hr) |
|---|---|---|---|---|---|---|---|---|---|---|
| Untreated | 27.0752 | 11.5625 | -0.572 | $5.148 \times 10^{-4}$ | 114 | $9.732 \times 10^{-7}$ | 0.55 | $1.914 \times 10^{4}$ | 0.2452 | $7.237 \times 10^{-6}$ |
| 0.10 | 30.9754 | 15.3125 | -0.559 | $4.701 \times 10^{-4}$ | 137 | $6.164 \times 10^{-8}$ | 0.62 | $4.834 \times 10^{4}$ | 0.1849 | $5.606 \times 10^{-6}$ |
| 0.25 | 35.2625 | 17.2125 | -0.550 | $4.232 \times 10^{-4}$ | 164 | $2.993 \times 10^{-8}$ | 0.71 | $6.236 \times 10^{4}$ | 0.1536 | $3.097 \times 10^{-6}$ |
| 0.50 | 38.7251 | 19.9875 | -0.528 | $3.818 \times 10^{-4}$ | 211 | $1.101 \times 10^{-8}$ | 0.82 | $1.512 \times 10^{5}$ | 0.1275 | $2.278 \times 10^{-6}$ |
| 0.75 | 40.5125 | 20.9125 | -0.520 | $3.547 \times 10^{-4}$ | 256 | $4.953 \times 10^{-9}$ | 0.87 | $6.781 \times 10^{5}$ | 0.1087 | $8.799 \times 10^{-6}$ |
| 1.00 | 71.5683 | 21.3375 | -0.495 | $3.079 \times 10^{-4}$ | 299 | $3.626 \times 10^{-9}$ | 0.89 | $8.846 \times 10^{6}$ | 0.0943 | $4.540 \times 10^{-7}$ |

**Entries were averaged over three measurements*

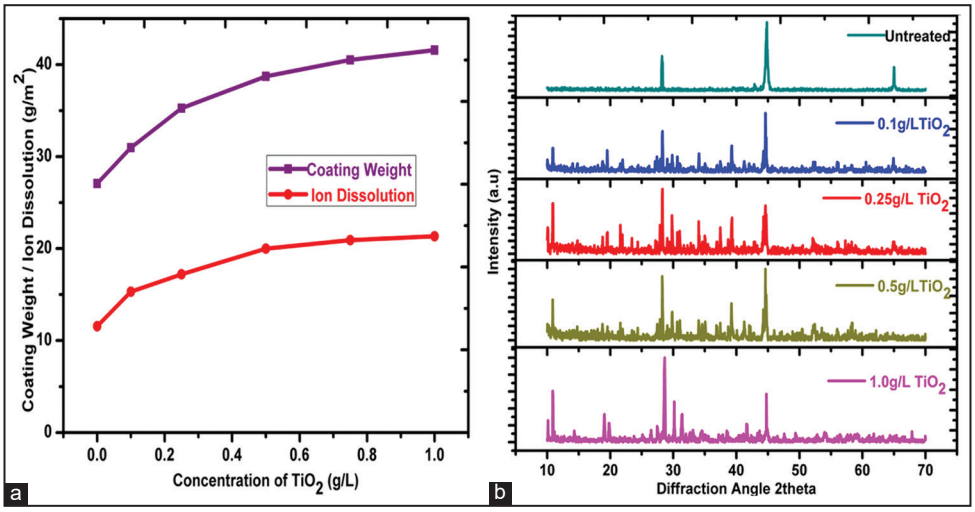


**Figure 1:** (a) Coating weight and Ion dissolution of $TiO_2$ assisted PCC coating, (b) X-Ray diffraction pattern of $TiO_2$ assisted PCC coating.

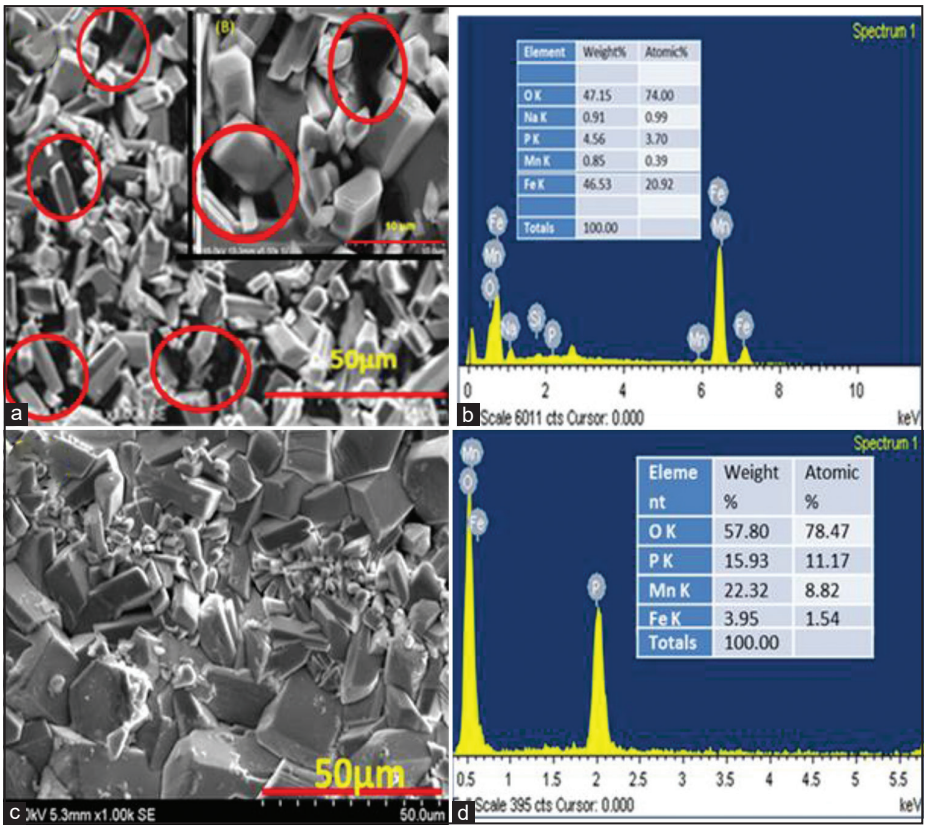


**Figure 2:** FESEM image and EDX analysis of $TiO_2$ assisted PCC coating. (a) Untreated, (b) Treated, (c) 1.0g/L $TiO_2$ (d) EDX

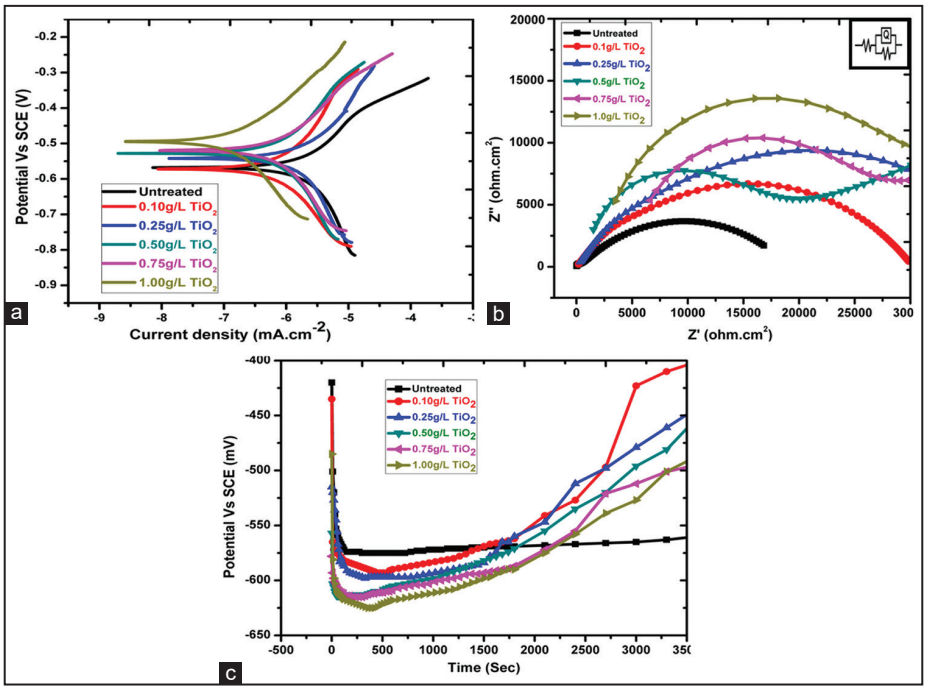


**Figure 3:** Electrochemical analysis of $TiO_2$ assisted PCC coating. (a) Potentiodynamic Polarization curves, (b) Nyquist plots (c) Potential-Time measurement.

elements is higher in treated samples, resulting the intense and uniform coating.

XRD pattern of additive-assisted PCC coatings is shown in Figure 1. It is obvious that manganese iron hydrogen phosphate hydrate referred as iron hureaulite $[(Mn,Fe)_5.H_2(PO_4)_4.4H_2O]$ (JCPDS, $2\theta \approx 28.51$), manganese phosphate hydroxide hydrate referred as manganese hureaulite $[Mn_5(HOPO_3)_2(PO_4)_2(H_2O)_4)]$, (JCPDS, $2\theta \approx 10.93$), $[Mn_5(PO_3(OH)_2(PO_4)_2(H_2O)_4)]$, (JCPDS, $2\theta \approx 41.35$), and manganese phosphate hydrate $[Mn_5(PO_4)_2[PO_3(OH)]_2{*}4H_2O]$ (JCPDS, $2\theta \approx 34.11$) is the predominant phases. However, EDX symbolized the presence of Ti due to residual coating with $Fe/Fe(OH)_3$. XRD pattern also reveals peaks concerning to iron [Fe (JCPDS, $2\theta \approx 65.31$)] and

iron hydroxide [$Fe(OH)_3$, (JCPDS, $2\theta \approx 45.05$)]. The presence of iron peaks confirms its codeposition along with manganese phosphate during the coating process. The additive leads to less porous coating whereas the untreated sample having more porous, acknowledged by the intense peak of Fe comparatively. Based on the mechanism and chemical compounds formed, coating material deposited on D2 steel could be denoted as iron-manganese phosphate composite.

### *3.3. Estimation of Anti-corrosion Performance*

The potentiodynamic polarization curves of coated samples, in 3.5% NaCl, are shown in Figure 3a. Cathodic corrosion inhibition takes place when coated samples were immersed in 3.5% NaCl. Higher concentration of additive (1 g/L) exhibits higher anodic shift Ecorr (corrosion potential) about −0.495V and it is relatively low for untreated sample about −0.572V. Meanwhile, the corrosion current densities (Icorr) decreased from about $5.148 \times 10^{-4}$ μA.cm$^{-2}$ of untreated sample to about $3.079 \times 10^{-4}$ μA.cm$^{-2}$ of higher concentration of additive, gradually. It is because of the surface coverage of base metal by composite coating which act as a barrier layer for the electron transfer process. Higher coating weight leads a high anodic shift in Ecorr and lowers the corrosion current density (Icorr) [7,9].

The Nyquist plots of coated samples in 3.5% NaCl, acquired at their respective OCPs, are shown in Figure 3b. The larger diameter of the semicircle indicated that the coating possess higher polarization resistance. In the Nyquist plots, high-frequency region exhibits a semicircle subsequently a typical Warburg impedance behavior at the low-frequency region for all treated samples indicating that the corrosion of coated samples is under diffusion control. Therefore, the electrical circuit placed in the inset of Figure 3b is used to fit the EIS data of coated samples. The obtained electrochemical parameters are composed in Table 1 where Rs is the solution resistance, CPE is a constant phase element which replaced the double layer capacitance ($C_{dl}$), and $R_1$ is the corresponding resistance of CPE. The inferences of EIS studies were the impedance of additive enhanced coatings which were relatively higher than the untreated sample.

### *3.4. Potential Time Measurement*

We have measured potential in a particular time intervals for coated samples using digital potentiometer, shown in Figure 3c. Initially, potential decreases and then it escalates gradually with time and achieves a steady state potential after ≈25 min of immersion. The time taken for attaining the steady state potential each concentration of additive differs. It indicates that initial dissolution of base metal is followed by the building of phosphate coating. Moreover, the key role of additive is accelerating the rate of dissolution of base metal and also facilitates the coating process. It helps to identify the actual time at which the effective coating occurred [11].

### *3.5. Corrosion Weight Measurement*

Corrosion weight per unit area can be calculated using mathematical expression [7] and corrosion rate (g.h$^{-1}$) produced by potentiodynamic polarization study is shown in Table 1.

$$W_{\text{corrosion weight}} = \frac{W_2 - W_4}{A} \text{ g / m}^2$$

Where, $W_2$ – weight of the phosphate sample, $W_4$ – weight of the sample after 24 h immersion in 3.5% NaCl, and A – the surface area of phosphate sample.

The phosphate coated samples were immersed in 3.5% NaCl solution for 24 h. Then, the samples were washed, dried, and weighed. As per the obtained values, corrosion takes place maximum in untreated sample and gradually decreases as increasing the additive concentration.

## 4. CONCLUSION

Titanium dioxide enhanced PCC coating concludes the following: Field emission scanning electron microscopy (FESEM) images indicate that the added additive significantly altered the size of crystals from ≈ 40 μm to ≈10 μm. EDX analysis represents that the higher percentage of Mn, Fe, O, and P elements in higher concentration of additive favors compact, denser, and less porous phosphate coating. XRD pattern endorses that the deposition is a composite of iron and various types of manganese phosphates. EIS and potentiodynamic polarization study indicate that the highest coating weight enables more corrosion resistance. Potential time measurement helps to track the phosphate coating construction and reveals the completion of coating process. Significantly, additive accelerates the rate of coating process and also provides more uniform, compact, denser, less porous, high corrosion resistant, and better protective layer in shorter time.

## 5. ACKNOWLEDGMENT

The authors acknowledge the Director, National Centre for Nano science and Nano Technology, University of Madras, Chennai, for offering FESEM and EDX analysis. The authors thank to the Department of Chemistry, Indian Institute of Technology-Madras, for XRD studies.

## 6. REFERENCES

1. S. Palraj, M. Selvaraj, P. Jayakrishnan, (2005) Performance of polymer blends on phosphated steel substrate, ***Progress in Organic Coatings***, **54**: 1-4.
2. K. Ogle, M. Wolpers, (2003) Phosphate conversion coatings. In: ***Metals Handbook***, Vol. 13, Materials Park, Ohio: ASM International, p712.
3. A. Uebleis, D. Weng, H. Boehni, (1994) ***Proceedings of the First Swiss Conference on Materials Research for Engineering Systems***, Sion: Technische Rundschau, p316.
4. L. Guangyu, N. L. Liyuan, J. Jianshe, J. Zhonghao, (2004) A black phosphate coating for C1008 steel, ***Surface and Coatings Technology***, **176**: 215.
5. M. Gavgali, I. Kaymaz, Y. Totik, R. Sadeler, (2002) Corrosion behavior of 90% Cu-10% Ni alloy at different rotation speeds, ***Corrosion Reviews***, **20**: 403-414.
6. Y. W. Yao, Y. Zhou, C. M. Zhao, Y. X. Han, C. X. Zhao, (2013) Preparation and corrosion resistance property of Molybdate conversion coatings containing SiO2 nanoparticles, ***Journal of The Electrochemical Society***, **160**: C185-C188.
7. M. Padma, S. Shanmugam, K. Ravichandran, (2020) Sodium silicate assisted manganese phosphate chemical conversion coating on D2 steel at various concentration, ***Surfaces and Interfaces***, **20**: 100547.
8. J. Wang, W. Zhou, Y. Du, (2012) Effect of sodium silicate pretreatment on phosphate layer: Morphology and corrosion resistance behavior, ***Materials and Corrosion***, **63**: 317-322.
9. S. Shanmugam, K. Ravichandran, T. S. N. Sankara Narayan, M. H. Lee, (2015) A facile electrochemical approach for the deposition of iron-manganese phosphate composite coatings on aluminium, ***RSC Advances***, **5**: 988-1008.
10. S. Jegannathan, T. K. Arumugam, T. S. N. Sankara Narayanan, K. Ravichandran, (2009) Formation and characteristics of zinc phosphate coatings obtained by electrochemical treatment: Cathodic vs. anodic. ***Progress in Organic Coatings***, **65**: 229-236.
11. C. Marikkannu, K. Balakrishnan, (1999) Investigation of phosphate coating formation by electrochemical impedance spectroscopy, ***Bulletin of Electrochemistry***, **15**: 156-159.

***Bibliographical Sketch***


M. Padma and K. Ravichandran are affiliated to Department of Analytical Chemistry, University of Madras, Guindy, Chennai, Tamil Nadu, India, Department of Chemistry, Bharathi Women's College, Chennai, Tamil Nadu, India